JOURNAL OF MATERIALS SCIENCE 33 (1998) 5383–5396

Influence of poly(acrylic acid) molar mass on the fracture properties of glass polyalkenoate cements

S. GRIFFIN*, R. HILL
Department of Material Science and Technology, University of Limerick, Plassey Park, Limerick, Ireland
E-mail: Robert.Hill@UL.IE

The failure behaviour of glass polyalkenoate cements was investigated using a linear elastic fracture mechanics (LEFM) approach. Cements were based on four model glasses with varying reactivity and four poly(acrylic acid)s (PAA)s with number average molar masses (M_n) ranging from 3.25×10^4 to 1.08×10^5. Cement properties were studied at time intervals of one, seven and twenty eight days. Compressive strengths (σ_c) of the cements increased with increasing fluorine content of the glass, with increased molar mass of the PAA and with ageing time. The Young's moduli increased with time, but were lower for cements based on the fluorine free glass. Moduli values were independant of PAA molar mass. The un-notched fracture strength (σ_f) of the cement increased with the molar mass of the PAA and with ageing time. Glass composition did not appreciably influence the un-notched fracture strength. The fracture toughness (K_{IC}) increased with the molar mass of the PAA and with ageing time, but reduced with increasing fluorine content of the glass. The toughness (G_{IC}) was dependant on molar mass. The influence of molar mass was not as great as predicted by the reptation chain pull-out model for fracture. The molar mass dependence of toughness was greatest with the lower fluorine content glasses. The plastic zone size at the crack tip increased with the molar mass of the PAA. However the plastic zone size decreased with ageing time for all the cements studied and was smaller for the more reactive higher fluorine content glasses.

1. Introduction

Glass polyalkenoate cements are formed by reacting powdered glasses with aqueous poly(acrylic acid). The acid degrades the glass structure and hydrolyses the bonds of the glass network. Aluminium-oxygen-silicon bonds [1] and phosphorous-oxygen bonds [2] of the glass network are hydrolysed releasing aluminium and calcium cations, which are chelated by the carboxylate groups and serve to "crosslink" the polyacrylate chains. In addition fluoride and phosphate anions are released and a silica based gel is formed. The setting reaction is shown schematically in Fig. 1.

The final cement consists of residual glass particles embedded in a polysalt matrix, which can be regarded both as a cement and a polymer composite (Fig. 2).

Hill *et al*. [3] have shown that these cements exhibit sharp loss peaks typical of thermoplastics. The molar mass of the poly(acrylic acid) used to form the cement exerts a significant influence on the mechanical properties of the cement [4–6] and in particular the toughness, indicating that the crosslinks are labile and that these cements have a thermoplastic character.

2. Fracture of thermoplastic polymers

Berry [7, 8] demonstrated that the measured fracture surface energy of a thermoplastic polymer was much greater than the energy required to break all the polymer chains crossing the crack plane. The high fracture surface energy was attributed to a localized flow process of polymer chains at the crack tip. Berry attributed the inherent Griffith flaw size found with polymers, such as poly(methylmethacrylate) to a plastic zone or craze that formed prior to catastrophic failure.

The strength of polymers is related to long range entanglements that serve to restrict chain motion. The early ideas of chain entanglements viewed the entanglement as a physical knot that served to limit chain slippage during fracture. However, polymer chains are too inflexible to form physical knots and a model has been developed [9] that views a chain as being trapped in a tube of entanglements formed by neighbouring chains. This model, known as reptation, is shown schematically in Fig. 3.

In the reptation model a chain is viewed as moving along an imaginary "tube" with a snake-like motion.

* *Present address*: Boston Scientific Ballyford Industrial Estate, Galway, Ireland.

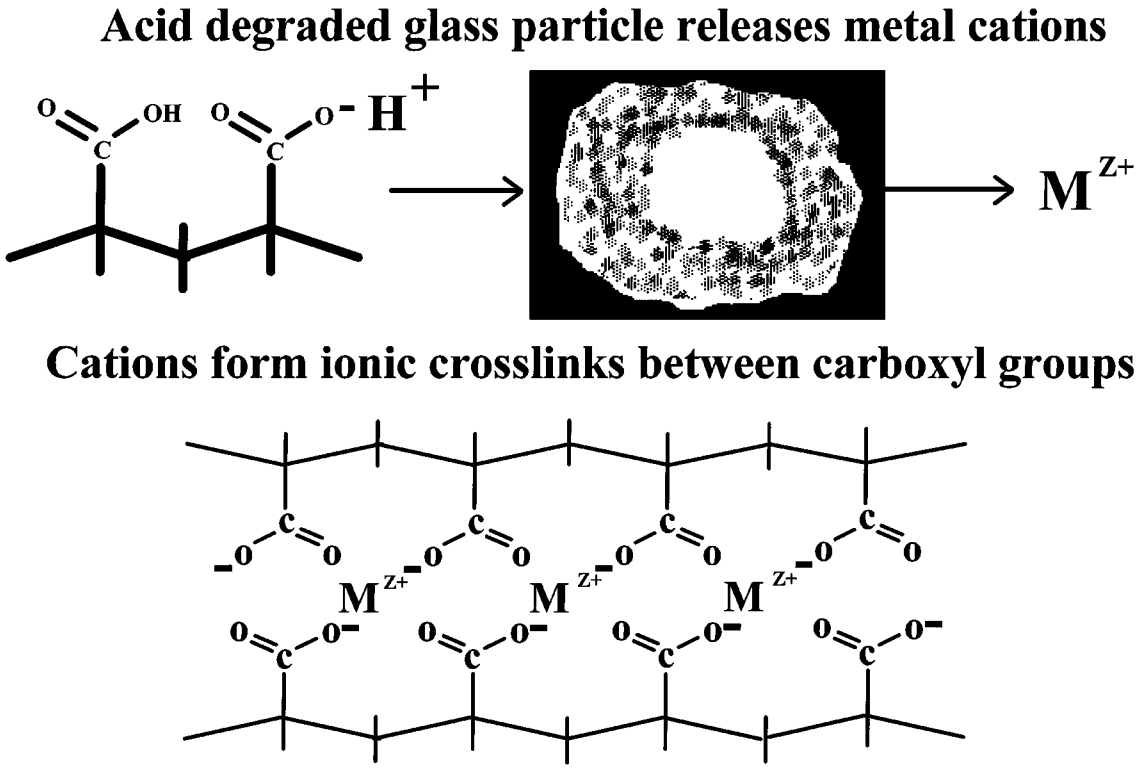

Figure 1 Schematic setting reaction of a glass polyalkenoate cement.

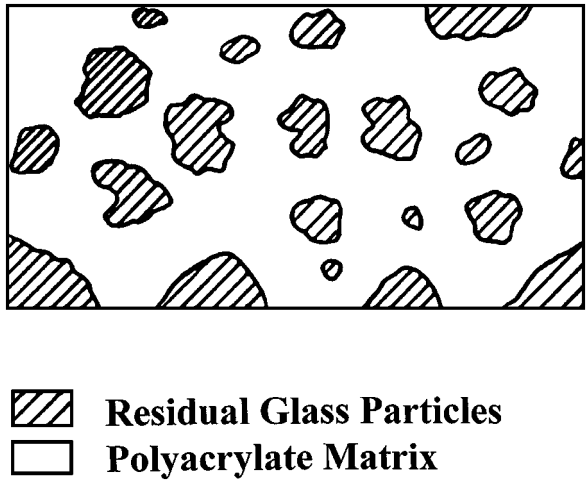

Figure 2 Composite nature of a glass polyalkenoate cement showing residual glass particles embedded in a polysalt matrix.

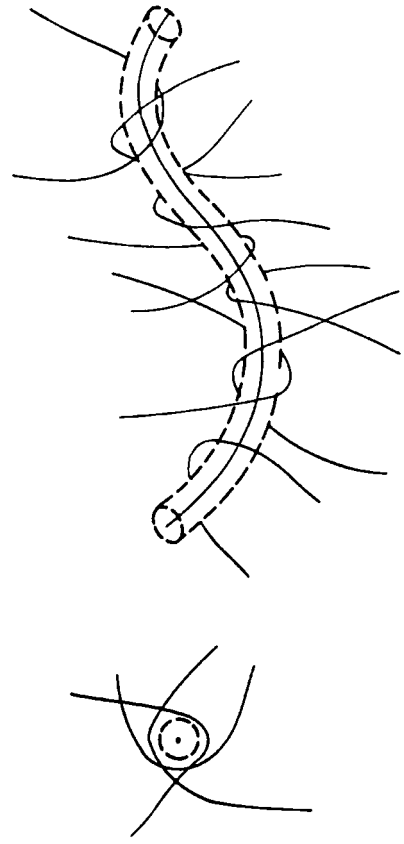

Figure 3 Reptation model showing a polymer chain trapped in a tube of entanglements.

The mobility of the polymer chain is restricted by the presence of entanglements, since in moving, one chain may not cross the contour of another. Longitudinal motion is also prevented by the interaction of substituents on neighbouring chains that give rise to potential barriers to chain mobility along the tube.

The dynamics of a polymer chain in a melt or concentrated solution have been described by the reptation model [9, 10]. This reptation model has also been used to describe fracture [11,12] and crack healing [13,14] in polymers.

The reptation/chain pull out model for fracture is shown schematically in Fig. 4. The following analysis is based on that of Prentice [15].

Using a simple power law viscous model it can be shown that the shear stress (τ) experienced by the chain in its tube will be proportional to the apparent strain rate (γ_a)

$$\tau = \mu(\gamma_a)^n \quad (1)$$

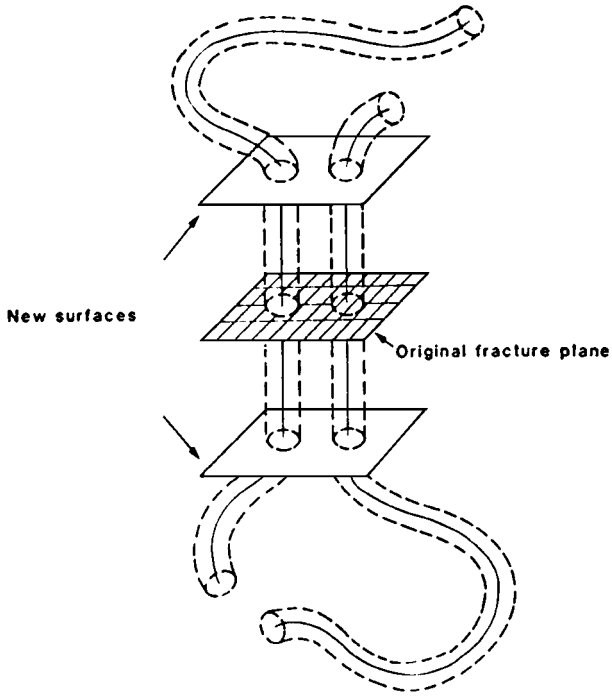

Figure 4 Reptation chain pull-out model of fracture.

where μ is a coefficient of viscosity resulting from the interaction between substituents on the extracted chain and the chains forming the tube. However

$$\tau = \frac{F}{A} \tag{2}$$

where F is the force acting on the end of the chain in the direction of the tube and A_s is the effective surface area of the tube occupied by the polymer chain

$$A_S = 2\pi r l \tag{3}$$

where r is the radius of the polymer chain, and l the contour length of the tube occupied by the polymer molecule.

The apparent strain rate may be defined by:

$$\gamma_a = \frac{V}{h} \tag{4}$$

where h is the spatial gap between the chain and the surface of its imaginary tube and V is the rate of removal of the chain.

Combining Equations 1 to 4 we obtain

$$F = \mu 2\pi r \left(\frac{V}{h}\right)^n l \tag{5}$$

The energy to extricate one chain from its tube is then

$$\tau_0 = \int_{l=0}^{l=L} F \, \mathrm{d}l \tag{6}$$

where L is the total contour length of the tube vacated, thus

$$\tau_0 = \int_{l=0}^{l=L} \mu 2\pi r \left(\frac{V}{h}\right)^n l \, \mathrm{d}l \tag{7}$$

At constant v

$$\tau_0 = \mu\pi r \left(\frac{V}{h}\right)^n L^2 \tag{8}$$

The fracture surface energy per unit area of fracture plane will then be:

$$\tau = \tau_0 N_s \tag{9}$$

where N_s is the number of segments crossing a unit area of crack plane. The assumption implies that a polymer chain only crosses the fracture plane once, which may be questionable, but considerably simplifies the analysis.

Combining Equations 8 and 9:

$$\tau = \mu\pi r N_s \left(\frac{V}{h}\right)^n L^2 \tag{10}$$

The equation implies that at a fixed crack opening velocity (V) the work done in removing chains from a unit area of crack plane is proportional to the molar mass squared.

$$\tau \propto M^2 \tag{11}$$

At some stage a molar mass will be reached where the stress to extricate a chain from its tube is greater than that required for homolytic chain scission of an extended segment.

A consequence of Equation 5 is that at a constant crack opening velocity a critical value of the force, F_c, will be reached at a critical chain length, l_c. Above this value of l_c the force required to pull out chains from their tubes will be greater than that to break the carbon-carbon bonds of the polymer backbone. Below this critical value (l_c) chain pull out will be the dominant mechanism and the fracture surface energy will be determined by Equation 10. Whilst above l_c chain scission will occur and the fracture surface energy will then be independent of molar mass.

Equation 11 requires further slight modification to account for the fact that there is also a critical molar mass, below which chains do not form entanglements. This results in the modification of Equation 11 to:

$$\tau \propto (M - M_c)^2 \tag{12}$$

where M_c is the molar mass required for entanglements to occur.

The critical molar mass is the value above which chain scission occurs and the toughness is no longer related to molar mass. The critical molar mass is typically about 10^5, however its value is generally lower, where there are strong inter-molecular interactions between polymer chains [16].

Toughness data is plotted as function of number average molar mass for poly(methyl methacrylate) in Fig. 5. At high molar masses above a critical value M_c, toughness is independent of molar mass. This is explained by the force to extricate a chain from its tube being greater

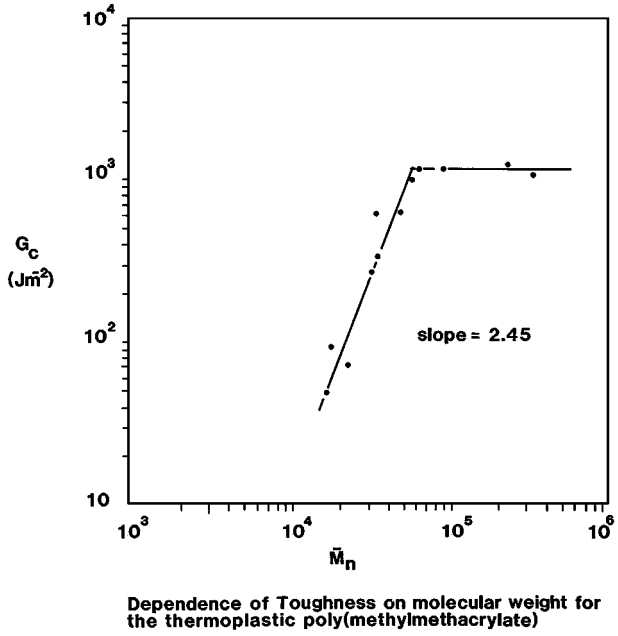

Figure 5 Plot of Log(G_{IC}) against Log (M_n) for poly(methylmethacrylate).

than that required to cause chain scission. Chain breakage then occurs and there is no further increase in toughness with molar mass. At low molar masses below approximately 2.7×10^4 the toughness goes to zero, since the chain length is too short to form entanglements and the tube concept no longer applies. At intermediate molar masses the slope of the log(toughness)-log(M_n) plot is about 2.45, slightly higher than the value of two, predicted by the reptation model. The entanglement molar mass (M_c) again varies from polymer to polymer, but in general corresponds to between 100 and 300 monomer units [17]. The monomer unit molar mass is 72 for PAA which gives and M_c of between 7000 and 21000.

3. Fracture of glass polyalkenoate cements

The application of a chain pull out model to the fracture of a glass polyalkenoate cement may be considered of doubtful value at first sight, however, experimental observations indicate that the crack propagates through the polymer matrix phase and not through the glass phase, thus fracture in these cements is essentially fracture of the polymer matrix phase.

The mechanical properties of glass polyalkenoate cements change with time as the setting reaction proceeds [6, 18–21]. Compressive and flexural strengths generally increase with time [18–20], but in some cases may also decrease with time [20, 21]. The changes in mechanical properties have generally been associated with increased crosslinking of the polyacrylate chains by cations, but recently Nicholson and Wasson [22] have put forward the idea that the changes are due to the formation of a silicate phase, rather than a continuing crosslinking reaction. This view has gained acceptance in the literature, and is supported by a number of recent studies [23–25]. Wilson [23] found evidence for cement formation with an aluminosilicate glass and acetic acid. Milne *et al.* [24] found evidence for phosphate and silicate species and Matusuya *et al.* [25] in an elegant study correlated increases in compressive strength with formation of a silicate phase by MAS-NMR. However the continued crosslinking reaction provides a better explanation of the observed data. For example the Young's moduli increase with time [6] and the cements become less viscoelastic in character with time [26], which is consistent with increased crosslinking of the polyacrylate chains. The toughness may increase or decrease with time [6] depending on the poly(acrylic acid) molar mass, which suggests that flow of the polyacrylate chains at the crack tip and the extent of plastic zone formation may be the dominant factors in determining the fracture properties. Decreases in toughness with time may be accounted for by excessive crosslinking, restricting flow of the polyacrylate chains and reducing the plastic zone size at the crack tip. However, the strongest argument against the idea that a silicate phase accounts for significant changes in cement mechanical properties is that cements based on silicate phases, such as Portland cement, or high alumina cement generally have very low toughness values, typically about 5 J m^{-2} compared to glass polyalkenoate cements that have toughness values normally in the range 50–100 J m^{-2}. The contribution of a silicate phase is therefore likely to be small. Furthermore transmission electron microscopy [27] shows the silicate phase to be located predominately at the periphery of the reacted glass particles and crack propagation takes place through the polysalt matrix [4]. Recently Matusuya *et al.* [28] have also investigated cements based on a very low molar mass poly(acrylic acid) of approximately 1000 molar mass and a slightly higher molar mass cements based on a molar mass of 5000. The low molar mass cement had a compressive strength of ≈ 5 MPa compared to the slightly higher molar mass cement of ≈ 33 MPa. This again indicates that it is the polymer component, which dominates the compressive strength and that the silicate phase contributes little to the strength and toughness.

Glass polyalkenoate cements are currently used as adhesives in dentistry and as anterior tooth fillings, liners and bases [29]. They are also being developed and used for medical applications, as a pre-set bone substitute and as a bone cement [30–32]. Four revision hip replacements and four revision knee replacements have been successfully carried out using glass polyalkenoate cements [33]. Glass polyalkenoate cements have many attractive properties, including the ability to wet and chemically bond to medical grade alloys, as well as the apatite phase of tooth and bone. They also have the ability to release fluoride ions, which have a cariostatic effect, and are known to stimulate osteoblast mitosis [34] and deposition of apatite [35]. However they lack the strength and fracture toughness required for use as a posterior dental filling material and as a bone cement in major joint replacement surgery. Current commercially available restorative grade glass polyalkenoate cements have fracture toughness values in the range 0.3–0.55 MPa m$^{1/2}$ [36–37].

Increased fracture toughness and plasticity at the crack tip would also be expected to increase their adhesive bond strength to enamel, since failure occurs

cohesively in the cement layer [38]. If the bond strength could be increased comparable to resin based adhesives, glass polyalkenoate cements would be more attractive for the bonding of orthodontic brackets to teeth.

Despite the low fracture toughness of these materials there have been few published studies of their fracture behaviour with view to understanding the parameters controlling the fracture process and improving their fracture toughness.

The objective of the present paper is to gain an understanding of the fracture behaviour of glass polyalkenoate cements. Previous published studies have been limited to cements based on commercial glasses [4–6]. In the present study cements based on four model glasses of varying reactivity were investigated. A recent study [6] has indicated that current glass polyalkenoate cements may exhibit poor toughness, because there are too many crosslinking ions in the matrix, which restricts plastic flow at the crack tip. The ability to control the reactivity of the glass should enable the extent of the crosslinking reaction in the polyacrylate matrix to be varied. Cements were formed with four poly(acrylic acid)s of varying molar mass and four glasses of varying reactivity. The properties of the resulting cements were studied, as a function of time, since the crosslinking reaction is thought to continue with time.

4. Experimental

4.1. Materials

4.1.1. Glass preparation

Glasses were prepared based on the following molar composition:

$$PSiO_2\text{-}QAl_2O_3\text{-}1.5P_2O_5\text{-}(5\text{-}X)CaO\text{-}XCaF_2$$

The reactivity of the glass was altered by switching two fluorines for one oxygen in the glass network. Introducing fluorine increase the glass reactivity by disrupting the glass network. The compositions were designed to eliminate fluorine loss from the melt as silicon tetrafluoride during firing [40].

The glasses were produced by mixing the appropriate amounts of silica $>99.99\%$ pure (Tilcon Industrial Minerals Stoke-on-Trent ST7 1TU UK)) with GPR grade alumina (BDH Poole BH15 1TD UK), calcium carbonate (E.Merck D-6100 Darmstadt GERMANY) and calcium fluoride (Aldrich Chemical Co Milwaukee WI53233 USA) and ball milling for one hour, whereupon the appropriate amount of GRR grade phosphorous pentoxide (BDH Poole BH15 1TD UK) was added and mixed in. The prefired batch was then placed in a high density sintered mullite crucible (Zedmark Refractories Earlsheaton Dewsbury UK) and fired at the appropriate temperature for two hours. The resulting melts were then shock quenched by pouring directly into water to produce glass frit. A 100 g of glass frit was then placed in a 150 mm grinding pot and ground for 14 minutes using a Gyro mill (Glen Creston, Wembley UK). The resulting powder was sieved using a 45 μm sieve and the fraction <45 μm was used in the preparation of the cements.

TABLE I Molar mass details of the poly(acrylic acid)s

Code	Source and batch code	M_n	M_w	PD
E5	Allied Colloids	3.25×10^3	9.41×10^3	2.9
E7	Allied Colloids	6.66×10^3	2.26×10^4	3.4
"E9"	AHC/Shofu	2.29×10^4	1.68×10^5	7.3
E11	Allied Colloids	1.08×10^5	2.63×10^5	2.4

4.1.2. Poly(acrylic acid)s

The poly(acrylic acid)s were supplied by Advanced Healthcare (Tonbridge Kent UK) and Allied Colloids (PO Box 38 Bradford UK). The relevant code letters and details are given in Table I. The poly(acrylic acid)s were dried and ground to give a fine powder with a particle size <90 μm.

4.1.3. Cement preparation

Cement samples were formed by mixing the glass powder with the poly(acrylic acid) in a weight ratio of 5:1 and then adding this mixture to water containing 10% m/v (+) tartaric acid, in a weight ratio of 4 : 1. This represents a glass powder to poly(acrylic acid) solution ratio of 2 : 1 with an acid concentration of 40% m/m. In addition, the compressive strength of the cements were also tested at a glass powder to poly(acrylic acid) ratio of 2.5 and with an acid concentration of 50% m/m.

4.2. Cement testing

Unless otherwise stated all tests were carried out in a water bath at 37 ± 2 °C. Compressive strength tests were additionally carried out in air at room temperature 19 ± 2 °C in accordance with the relevant ISO standard [41].

The compressive strength of cements based on nine glasses were investigated initially. Four of these glasses were then selected for further study and cements based on them were characterised using a Linear Elastic Fracture Mechanics approach.

4.2.1. Compression test

The compression tests were performed on cement cylinders 4.0 mm in diameter by 6.0 mm in height. The testing procedure was based on the ISO ISO7489: "1986 Dental Glass Polyalkenoate Cements" [41]. An Instron Universal tensometer (Instron High Wycombe Bucks UK) was used for the test at a crosshead displacement rate of 1 mm min^{-1}.

The test was carried out on 8 samples and the compressive strength calculated according to:

$$\sigma_c = F/\pi r^2 \tag{13}$$

where σ_c is the compressive strength, F is the force in Newtons and r is the diameter.

In addition a 0.5% offset yield stress was determined for the compressive tests carried out at 37 °C in water.

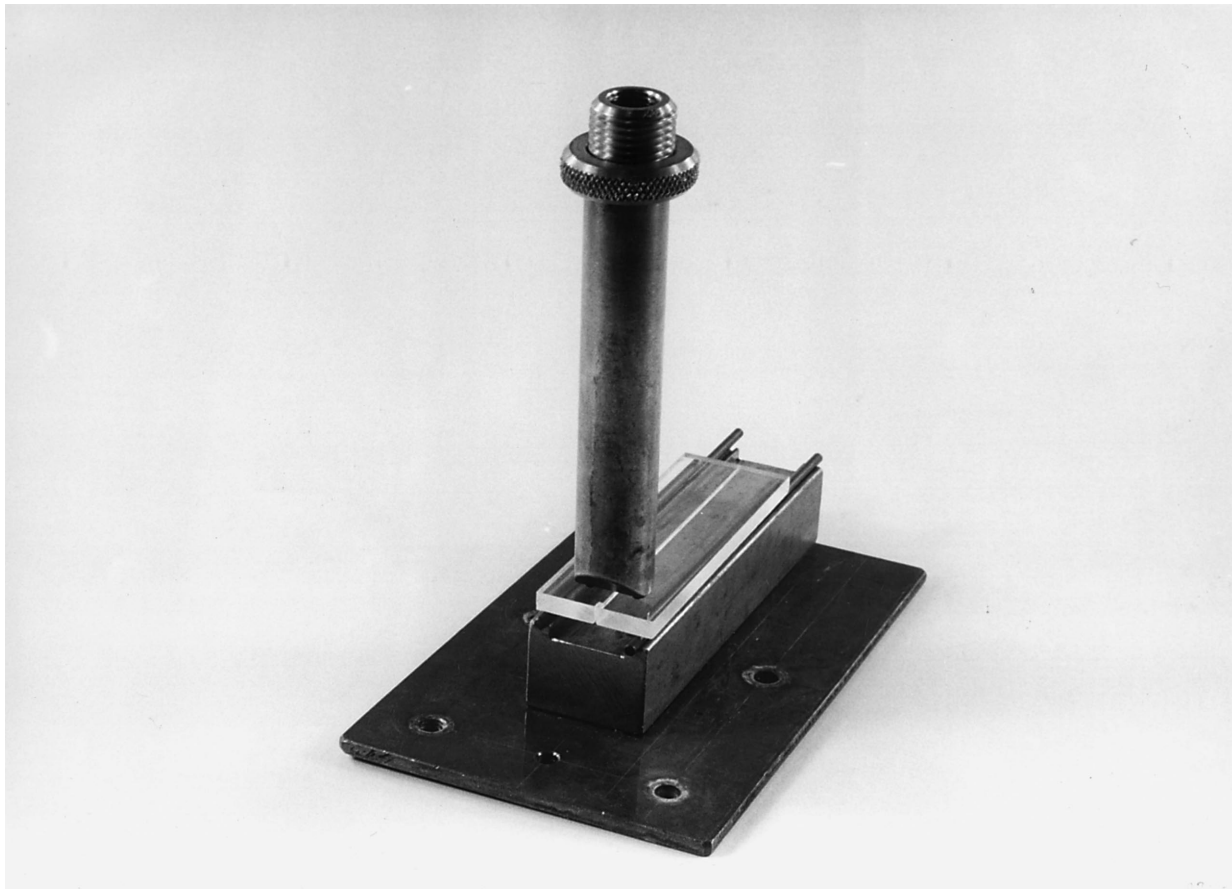

Figure 6 A double torsion testpiece and test fixture.

4.2.2. Double torsion test

DT specimens $3.5 \times 65 \times 25$ mm (Fig. 6) were produced as described previously in the form of rectangular plates. Double torsion specimen blanks were moulded from the appropriate cement pastes using a 3.00 mm thick stainless steel former with two stainless steel backing plates. Cement paste was placed in the former and the backing plates placed over the former. The two backing plates were held in position by a G clamp and excess cement paste eliminated. The cement pastes were allowed to set at 37 °C for one hour and then removed from the mould and stored in water at 37 ± 2 °C prior to testing. A sharp groove was milled down the centre of one face of each specimen about 0.8 mm in width and 0.5 mm deep. A swallow tail, was cut into one end of the groove to facilitate pre-cracking. Pre-cracking was performed in the test jig by applying load with an Instron Universal Tensometer at a crosshead speed of 1 mm min^{-1} with rapid unloading once crack initiation took place. During the test the specimen was supported on a pair of parallel rollers of 2 mm diameter and spaced 20.0 mm apart. The load was applied at a constant rate of 0.1 mm min^{-1} to the swallow tailed end of the specimen via two ball bearings spaced 10.0 mm apart. The specimen was subjected to a four point bend during which the crack initiated and propagated along the groove.

The specimen dimensions and groove depth were selected to eliminate the need for crack shape correction factors to be applied [42].

In the double torsion test the mode I stress intensity factor K_I is independent of crack length and is given by Kies and Clark [43] as:

$$K_I = P_c W_m \left(\frac{3(1+\nu)}{W t^3 t_n} \right)^{1/2} \tag{14}$$

Where W_m is the moment arm, W is the specimen width, t is the specimen thickness and t_n the thickness in the plane of the crack and ν the Poission's ratio which was assumed to be 0.33. Values for K_{IC} were obtained for continuous fracture by substituting the load P_c and specimen dimensions into Equation 14.

4.2.3. Three point bend test

The Young's modulus, E and un-notched fracture strength, σ_f of each cement at the three time intervals were determined using a three point bend test, performed with the Instron tensometer. The relationship between the applied load, P and the displacement, δ at the centre of a specimen of rectangular cross section is:

$$P = \frac{4\delta E b t^3}{s^3} \tag{15}$$

where t is the specimen thickness, W the width of the specimen and S the distance between the supports. The test was carried out in accordance with ASTMS

D790-71 [44]. A span of 50 mm was used with a specimen size of 65 mm $\times$ 10 $\pm$ 0.03 mm $\times$ 3 $\pm$ 0.03 mm.

The Young's modulus was calculated from the initial slope of the plot of P against δ plot.

The un-notched fracture strength, σ_f is given by:

$$\sigma_f = \frac{3P_S}{2bt^2} \tag{16}$$

where P is the load at fracture.

A minimum of six specimens were tested for each test condition. Any specimens that were not visually flaw free were discarded prior to testing.

4.3. Calculation of the strain energy release rate (G_1) from DT specimens

The strain energy release rate was calculated assuming that pure linear elastic fracture mechanics apply using the following expression:

$$G_1 = \frac{K_1^2(1-\nu^2)}{E} \tag{17}$$

4.4. Calculation of plastic zone size

The plastic zone size, R_p was calculated from the fracture toughness and the 0.5?% offset yield stress determined from the compression test as follows:

$$R_p = K_{IC}^2/\sigma_{YS} \tag{18}$$

5. Results and discussion

5.1. Molar mass

The molar mass details in terms of number average molar mass, M_n and weight average molar mass, M_w and polydispersity, PD are given in Table I. The full molar mass distributions are shown in Fig. 7. The mercaptan free medical grade polymer E9 had a much broader molar mass distribution than the other three polymers and exhibits a double maxima in its molar mass distribution. This is believed to be due to the use of isopropanol as a chain transfer agent in the polymerisation process.

5.2. Compressive strength

The results for the compressive strengths determined in air at room temperature for the low formulation cements are shown in Table II and the results for the high formulation cements are shown in Table III. The compressive strengths generally increase with cement storage time. The compressive strength is dependant on the reactivity of the glass and the fluorine content. The compressive strength is significantly lower for the cements made with glasses containing no fluorine, or with low fluorine contents for both cement formulations. The increased glass content and polymer concentration results in a markedly higher compressive strength. For example the compressive strength increases from 101 to 201 MPa for the cements based on the $X = 2.0$ glass tested after one day.

TABLE II Compressive strength of low formulation cement produced with the E9 poly(acrylic acid)

	1 Day		7 Days		28 Days	
X	σ_c (MPa)	SD ($n=8$)	σ_c (MPa)	SD ($n=8$)	σ_c (MPa)	SD ($n=8$)
0	42.79	2.16	53.35	3.29	56.59	4.78
1.0	73.39	3.46	94.54	5.80	86.84	7.26
1.5	90.17	4.61	84.73	4.14	95.76	5.14
2.0	101.42	5.70	121.84	4.45	101.50	10.19
2.2	90.9	2.57	103.70	7.77	110.81	4.72
2.4	85.67	5.03	99.11	5.37	98.8	3.74
2.6	71.27	5.83	94.75	6.79	104.23	7.36
2.8	77.24	3.23	97.32	5.17	98.78	7.09
3.0	87.28	3.83	95.54	9.38	97.58	4.83

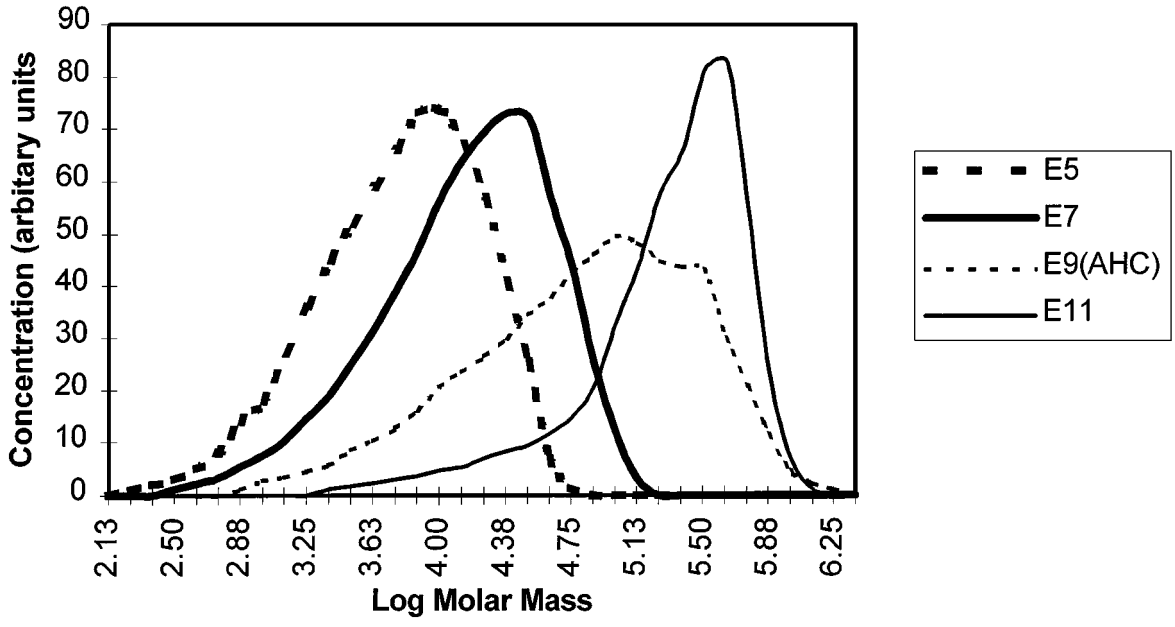

Figure 7 Molar mass distribution of the poly(acrylic acid)s studied.

TABLE III Compressive strength of high formulation cement produced with the E9 poly(acrylic acid)

	1 Day		7 Days		28 Days	
X	σ_c (MPa)	SD ($n=8$)	σ_c (MPa)	SD ($n=8$)	σ_c (MPa)	SD ($n=8$)
0	74.26	5.00	63.44	2.87	81.19	4.54
1.0	164.95	10.91	144.15	2.98	165.9	9.37
1.5	159.74	7.27	168.53	9.86	176.61	7.12
2.0	200.61	17.56	191.08	8.1	185.28	9.1
2.2	203.28	7.88	168.09	5.22	190.5	13.75
2.4	201.12	6.14	175.94	10.00	193.39	12.51
2.6	193.00	8.79	176.57	3.41	186.86	7.88
2.8	195.03	8.58	181.69	10.37	198.55	7.44
3.0	190.51	7.85	175.59	7.74	185.1	5.76

TABLE IV Compressive strengths measured in water at 37 °C for low glass content cements

		1 Day		7 Days		28 Days	
X	PAA	σ_c (MPa)	SD ($n=8$)	σ_c (MPa)	SD ($n=8$)	σ_c (MPa)	SD ($n=8$)
0	E5	19.53	1.05	29.8	0.62	31.62	1.36
1	E5	42.63	2.14	44.8	0.49	51.28	2.18
2	E5	45.37	1.72	53.18	3.13	54.56	2.71
3	E5	48.84	3.46	60.06	4.4	69.09	5.29
0	E7	26.61	2.54	37.3	0.48	41.44	1.43
1	E7	53.75	3.16	55.85	1.74	60.47	2.53
2	E7	57.97	2.64	68.45	1.2	65.91	4.12
3	E7	58.31	0.67	71.39	2.44	81.81	1.77
0	E9	34.02	2.48	46.21	0.95	47.87	0.41
1	E9	54.84	1.61	64.52	4.37	63.07	2.24
2	E9	68.18	3.46	86.12	3.48	87.38	4.37
3	E9	68.79	2.06	86.16	7.51	93.58	2.79
0	E11	44.15	3.17	52.78	4.68	60	4.71
1	E11	70.33	3.7	72.63	7.94	89.85	4.86
2	E11	79.05	3.98	84.31	1.75	98.62	4.87
3	E11	80.77	4.39	97.85	2.12	97.94	5.62

Increasing the test temperature to 37 °C and testing in water reduces the compressive strength significantly (Table IV) and results in increased plastic deformation behaviour. For example the compressive strength reduces form 101 to 68 MPa for the cement tested at 1 day based on the $X = 2.0$ glass on testing in water at 37 °C as opposed to testing in air at room temperature.

The compressive strength again increases with cement storage time. The molar mass of the poly(acrylic acid) has a significant influence on the compressive strength obtained. For example, when tested after one day the compressive strength is 49 MPa for a cement made with the $X = 3$ glass and a poly(acrylic acid) with $M_n = 3.23 \times 10^3$, but 81 MPa for a cement made with a polyacrylic acid with $M_n = 1.08 \times 10^5$. The molar mass and the glass type used in the cement were found to exert a significant influence on the amount of plastic deformation that took place prior to fracture. Cements made with the more reactive fluorine rich glasses and low molar mass poly(acrylic acid)s exhibited little plastic deformation prior to fracture. In contrast, cements made with the high molar mass poly(acrylic acid) E11 and the less reactive fluorine free glass exhibited marked plastic deformation. The amount of plastic deformation that took place prior to fracture was observed to reduce with cement storage time, consistent with increased crosslinking of the polyacrylate chains.

5.3. Young's moduli

The Young's moduli are shown in Fig. 8. The values given are the average values for the different poly(acrylic acid) molar masses studied. The experimental scatter on the Young's moduli values were relatively large and obscured any small differences being

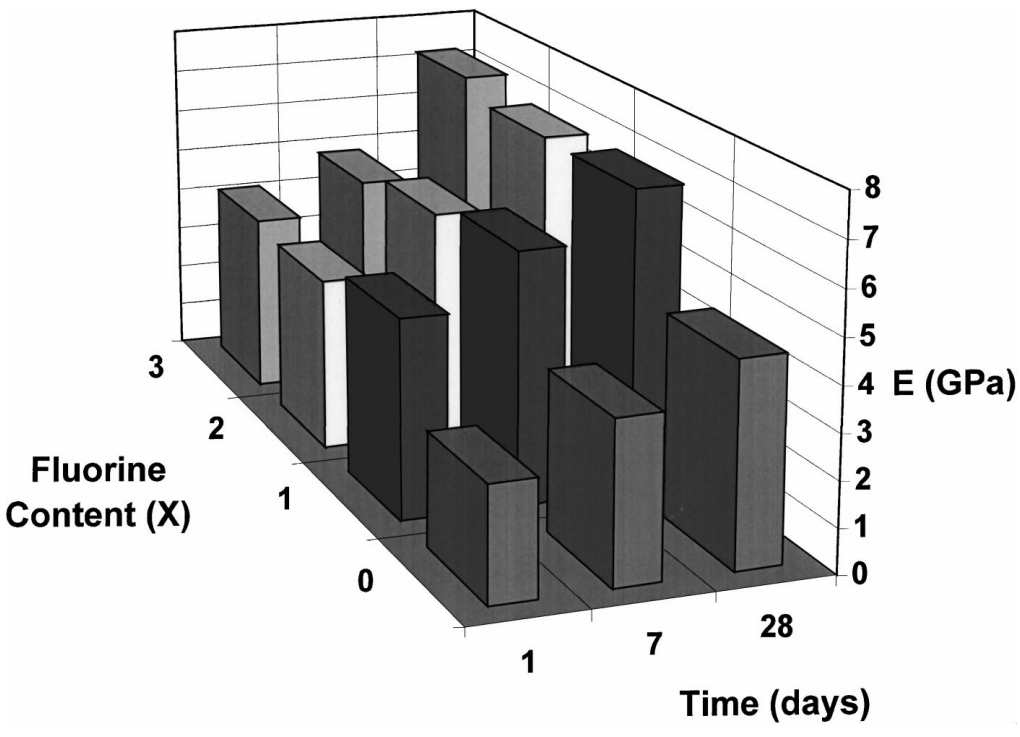

Figure 8 Averaged Young's moduli as a function of fluorine content of the glass and cement ageing time.

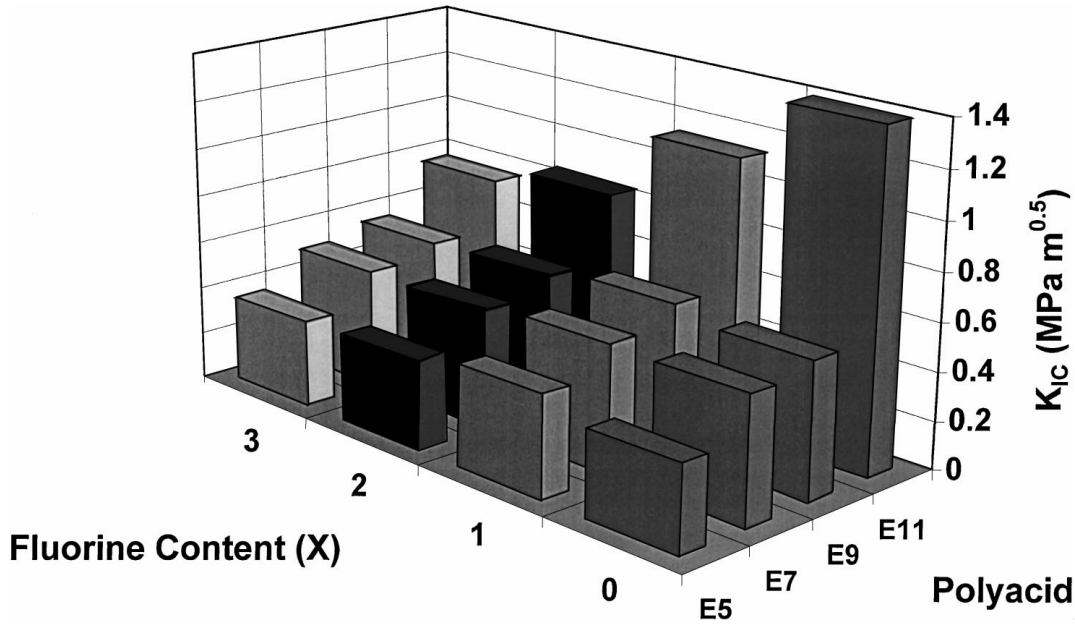

Figure 9 Fracture toughness values measured at 28 days for cements as a function of the fluorine content of the glass and poly(acrylic acid) molar mass.

detected between the fluorine containing glasses, however cements based on the non fluorine glass exhibited significantly lower moduli values at all time intervals and at all molar masses.

The fact that the fluorine containing glasses all have very similar moduli is surprising given the influence fluorine has in disrupting the glass network and its marked influence on glass reactivity and setting and working times of the cement pastes [45]. Solid state MAS-NMR results indicate that fluorine is exclusively bound to aluminium in the glass network [46]. Aluminium cations in the glass network that have a fluorine bound to them are more likely to be released from the glass than aluminium ions without a bound fluorine, since fewer chemical bonds will need to be broken to release such an aluminium fluorine complex. Thus the concentration of aluminium-fluorine complexes could be much higher in the cement matrix than in the glass and similar for all the fluorine containing glasses. Fluorine would be expected to inhibit ionic crosslinking and reduce the Young's modulus, however if the chance of forming a triple crosslink is remote, the hydrogen bonding ability of fluorine could help stabilise the aluminium carboxylate complexes and increase the effective crosslinking of the polyacrylate matrix.

The Young's modulus has previously [4, 6] been shown to be independent of molar mass and this would be expected to be the case with the present cements. The Young's moduli however all increase with time, which is consistent with the cement reaction continuing and resulting in increased crosslinking of the cement matrix. The previous study [6] also demonstrated the modulus to increase with time. The Young's moduli after 28 days are within the 7–13 GPa range for dentine and 7–20 GPa for cortical bone, which is important for good stress transfer between the cement and the appropriate tissue.

5.4. Fracture toughness

Table V gives the results of the fracture toughness tests and the results measured at one day are also plotted graphically in Fig. 9. The fracture toughness increases with molar mass for all the glasses studied and at all three time intervals. The fracture toughness generally increases with decreasing fluorine content of the glass and decreased glass reactivity. This supports the view that the existing commercial cements may be over crosslinked. In the present commercial materials based on poly(acrylic acid), a molar mass distribution close to that of the E9 material would typically be used in conjunction with a high fluorine glass similar to the $X = 3$ composition. The values for the fracture toughness of

TABLE V Fracture toughness values

		1 Day		7 Days		28 Days	
X	PAA	K_{IC} (MPa $m^{1/2}$)	SD ($n = 9$)	K_{IC} (MPa $m^{1/2}$)	SD ($n = 9$)	K_{IC} (MPa $m^{1/2}$)	SD ($n = 9$)
0	E5	0.27	0.01	0.36	0.01	0.35	0.01
1	E5	0.41	0.02	0.43	0.03	0.42	0.02
2	E5	0.28	0.01	0.33	0.01	0.37	0.01
3	E5	0.3	0.02	0.39	0.01	0.36	0.01
0	E7	0.47	0.01	0.51	0.02	0.52	0.03
1	E7	0.52	0.02	0.50	0.02	0.53	0.02
2	E7	0.37	0.01	0.41	0.01	0.49	0.02
3	E7	0.4	0.03	0.45	0.05	0.5	0.01
0	E9	0.57	0.02	0.6	0.06	0.56	0.02
1	E9	0.54	0.01	0.60	0.02	0.61	0.06
2	E9	0.51	0.04	0.55	0.02	0.56	0.03
3	E9	0.41	0.01	0.56	0.03	0.55	0.02
0	E11	1.13	0.06	1.24	0.05	1.39	0.06
1	E11	0.98	0.04	1.1	0.02	1.13	0.05
2	E11	0.71	0.06	0.85	0.03	0.84	0.01
3	E11	0.68	0.06	0.78	0.03	0.76	0.04

the current commercial cements are typically 0.4–0.55 MPa $m^{1/2}$, which is what would be expected for such cements based on the present paper.

The cements made with the lower fluorine content glasses and high molar mass poly(acrylic acid) E11 and E9 exhibit fracture toughness values higher than existing commercial materials. The highest fracture toughness value obtained was 1.39 MPa $m^{1/2}$ with the longest chain length poly(acrylic acid) and with the lowest fluorine glass. This value represents an almost three fold improvement on the values obtained from the existing commercial materials. Furthermore the fracture toughness values obtained are higher than the low copper, non γ'' amalgams and comparable with many existing dental composite resins. However, the fracture toughness is still significantly below that of the major phase of tooth, dentine at ≈ 2.4 MPa $m^{1/2}$.

Cements made with the E9 polymer are generally much closer in their fracture toughness values to the cements made with the E7 polymer, which is probably a result of the broader distribution of chain lengths in the E9 poly(acrylic acid) and the low molar mass tail that is also present.

The toughness or mode I critical stain energy release rate values are given in Table VI and the results measured at one day are plotted in Fig. 10. The toughness is greatest for the highest molar mass poly(acrylic acid), E11 with the least reactive glass, $X = 0$ at the shortest time interval studied of 1 day.

TABLE VI Toughness values

	E5 G_{IC} (J m^{-2})	E7 G_{IC} (J m^{-2})	E9 G_{IC} (J m^{-2})	E11 G_{IC} (J m^{-2})
$X = 3$				
1 day	19	29	21	100
7 days	28	38	58	74
28 days	16	31	37	71
$X = 2$				
1 day	18	23	34	114
7 days	18	28	51	93
28 days	17	31	41	92
$X = 1$				
1 day	23	37	49	167
7 days	29	39	56	158
28 days	23	42	38	190
$X = 0$				
1 day	25	55	64	446
7 days	32	65	89	303
28 days	24	53	62	381

5.5. Unnotched fracture strength

The un-notched fracture strength increases significantly with poly(acrylic acid) molar mass and with cement ageing time (Table VII and Fig. 11). However, the influence of glass composition is less marked. The lack of correlation between the fracture toughness and the flexural strength must arise from an increase in the inherent Griffith flaw size as the molar mass is increased. This may reflect the fact that the cement pastes became more difficult to mix as the molar mass of the poly(acrylic acid) was increased and the increased viscosity resulted in a small number of entrapped air bubbles.

The un-notched fracture strength values are comparable with the highest values found for commercially available glass polyalkenoate cements. Generally much smaller test specimen are used for determining the un-notched fracture strength of glass polyalkenoate cements than have been used in the present study. The use of a smaller specimen would be expected to increase significantly the strength values obtained.

5.6. Plastic zone size

The calculated plastic zone sizes are shown in Table VIII and plotted in Fig. 12 for the cements tested

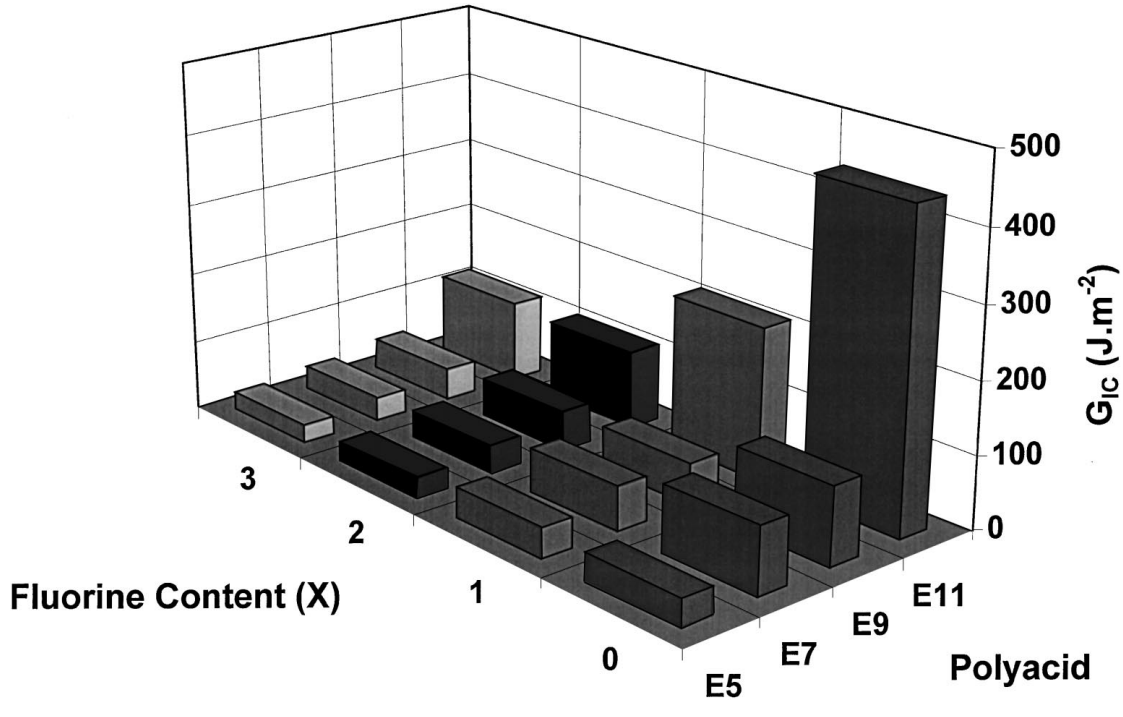

Figure 10 Toughness values measured at one day for cements as a function of the fluorine content of the glass and poly(acrylic acid) molar mass.

TABLE VII Un-notched fracture strength

		1 Day		7 Days		28 Days	
X	PAA	σ_f (MPa)	SD ($n=6$)	σ_f (MPa)	SD ($n=6$)	σ_f (MPa)	SD ($n=6$)
0	E5	6.1	0.13	6.33	0.86	9.01	0.75
1	E5	10.9	0.84	8.52	0.96	11.78	1.13
2	E5	5.8	0.45	5.84	0.48	8.42	0.62
3	E5	7.4	0.31	6.29	0.42	10.11	0.86
0	E7	10.57	0.56	10.13	1.49	13.76	0.14
1	E7	14	1.07	12.27	1.44	15.7	1.24
2	E7	9.38	1.02	8.91	1.16	8.92	1.12
3	E7	10.5	1.12	7.75	1.14	11.91	0.66
0	E9	13.9	0.12	15.05	0.67	17.48	2.05
1	E9	14.36	1.32	20.07	1.37	25.16	2.05
2	E9	17.05	0.65	16.7	1.3	17.8	1.37
3	E9	15.66	0.92	10.39	1.6	19.12	0.67
0	E11	20.21	1.47	21.03	1.9	28.74	1.04
1	E11	22.5	0.36	27.4	1.8	31.13	2.9
2	E11	20.8	0.75	23.93	1.63	30.86	3.26
3	E11	19.31	1.32	19.05	1.74	30.63	1.34

TABLE VIII Plastic zone size

		1 Day		7 Days		28 Days	
X	PPA	R_p (μm)	SD ($n=8$)	R_p (μm)	SD ($n=8$)	R_p (μm)	SD ($n=8$)
0	E5	17.0	1.7	12.0	0.08	12	0.7
1	E5	9.2	0.5	2.4	0.5	6	0.8
2	E5	2.4	0.3	2.6	0.1	2	0.3
3	E5	2.0	0.3	2.6	0.2	1.5	0.1
0	E7	54	5.9	23	1.2	16.0	0.22
1	E7	9.9	0.9	8.1	0.4	9.0	0.4
2	E7	3.2	0.1	2.7	0.3	3.0	0.3
3	E7	3.1	0.3	2.6	0.1	2.0	0.1
0	E9	42.5	3.5	19	1.6	15	0.6
1	E9	13	0.6	12	0.9	13	0.5
2	E9	5.4	0.5	4.7	0.2	4.0	0.1
3	E9	3.3	0.1	4.2	0.5	2.0	0.1
0	E11	212	25	175	1.5	117	12.7
1	E11	42.3	3.91	31	0.2	24	2
2	E11	16.2	1.6	19	0.1	9	0.4
3	E11	8.7	0.8	7.5	0.1	7	0.7

at one day. In all cases the plastic zone size was much less than the specimen thickness of 3.0 mm and it can therefore be concluded that all the double torsion specimens were being tested in predominantly plain strain conditions.

The plastic zone size increases with the poly(acrylic acid) molar mass and generally decreases with cement age and increasing fluorine content. The most marked reduction of plastic zone size with time was found for cements made with the highest molar mass poly(acrylic acid) and the fluorine free glass, where the plastic zone reduces from 212 μm at 1 day to 117 μm after 28 days. This is consistent with glass polyalkenoate cements undergoing further ionic crosslinking of the polyacrylate chains with time and the crosslinking process, restricting the amount of molecular flow taking place at the crack tip.

The largest plastic zone size of 212 μm was found for the cement with the highest poly(acrylic acid) molar mass and the least reactive glass, $X=0$ at the shortest time period studied. The smallest plastic zone size of 1.5 μm was found for the cement produced with the most reactive glass, the $X=3$ with the lowest poly(acrylic acid) molar mass at the longest time period studied. The plastic zone sizes obtained for the cements made with the fluorine free glass are larger than the values obtained

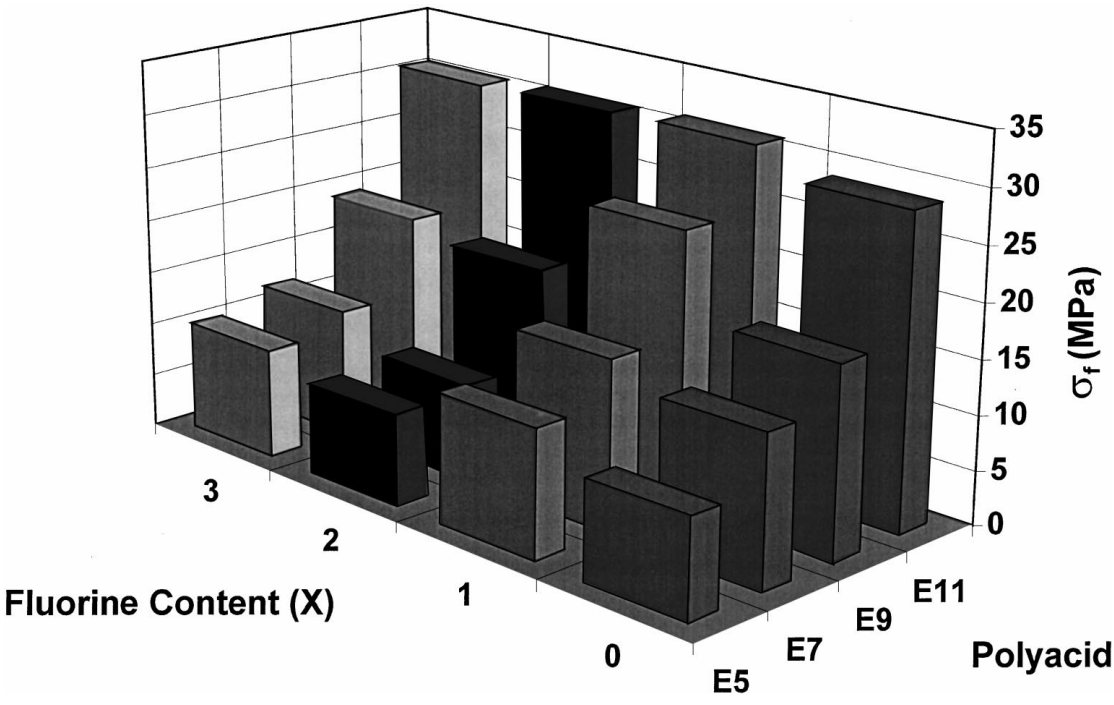

Figure 11 Un-notched fracture strength values measured at 28 days for cements as a function of the fluorine content of the glass and poly(acrylic acid) molar mass.

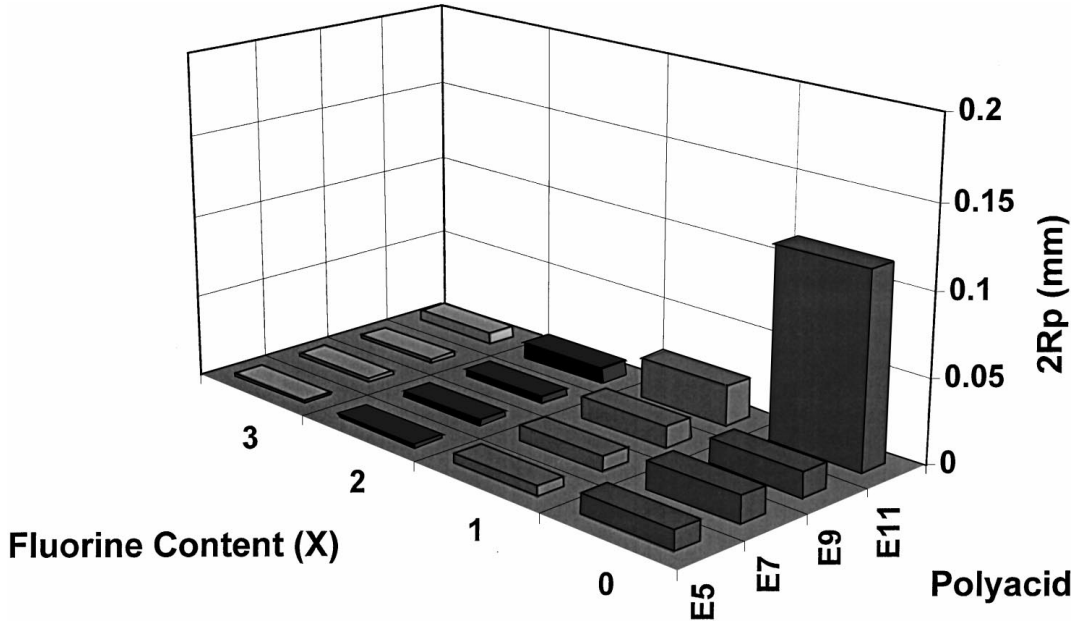

Figure 12 Plastic zone size values measured at one 28 days for cements as a function of the fluorine content of the glass and poly(acrylic acid) molar mass.

for the glass polyalkenoate cements and zinc polycarboxylate cements studied by Akinmade and Hill [39]. The results are consistent with increased crosslinking inhibiting molecular flow at the crack tip and reducing the plastic zone size.

5.7. Toughness

Previous studies of the influence of poly(acrylic acid) molar mass on the toughness of glass polyalkenoate [4, 6] and the related zinc polycarboxylate cements [47] have used a chain pull-out model developed for thermoplastic polymers [15] to analyse the data. As discussed previously, this model predicts the toughness to be dependant on the molar mass squared. However plots of log toughness against Log M_n gave a slopes of 0.5 and 0.8 for glass polyalkenoate and zinc polycarboxylate cements [4, 47], respectively. The reduction in slopes compared to that predicted theoretically and found experimentally for polymers, such as poly(methylmethacrylate) and polycarbonate was attributed to the presence of the weak ionic crosslinks between the chains. It is also important to note that in the chain pull-out model, the assumption that a single polymer chain can bridge the growing crack tip is incorrect. It is likely that the number of chains involved in fracture will not be simply the number of chains crossing the crack plane, but will include chains some short distance from the fracture plane. The number of chains involved in fracture might be expected to be proportional to the crack opening displacement, or plastic zone size.

A typical plots of log (toughness) against molar mass is shown in Fig. 13 and the results are tabulated in Table IX. The greatest slopes are found for the least reactive glass for the shortest time period studied at one

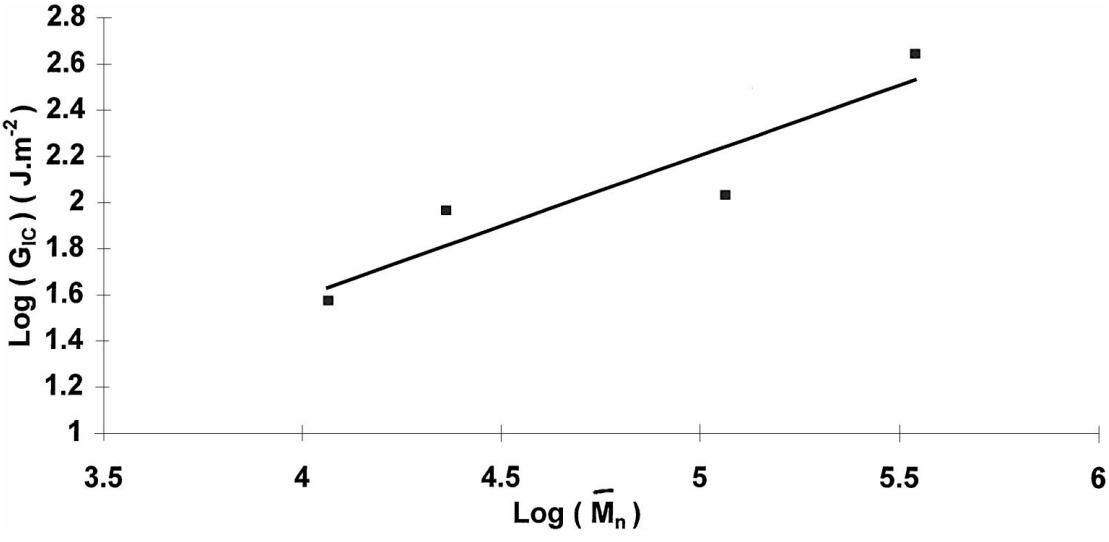

Figure 13 Typical Log(G_{IC}) against Log(M_n) plot.

TABLE IX Values for the slopes of the log toughness-log number average molar mass plots

	1 Day		7 Days		28 Days	
X	Slope	r^2	Slope	r^2	Slope	r^2
0	0.80	0.93	0.63	0.97	0.76	0.93
1	0.49	0.89	0.50	0.99	0.56	0.97
2	0.54	0.95	0.48	0.98	0.46	0.97
3	0.44	0.88	0.29	0.94	0.40	0.93

day, where a slope of 0.79 was obtained. This value is below that for thermoplastic polymers of 2.0 predicted by the reptation chain pull-out model. The smallest slope of 0.40 was found for the most reactive glass for the longest time period studied after 28 days.

The intercept on the x axis corresponds to a molar mass of about 100. In thermoplastics this value would be much higher and would typically correspond to a molar mass of between 5000 and 30,000 and correspond to the critical molar mass for the formation of chain entanglements. Below this molar mass, the polymer chains are no longer constrained by a tube of entanglements and the toughness would be zero. The intercept on the x axis for the present cements is at such a low value that it could not possibly correspond to the critical molar mass for the formation of entanglements, however it does correspond approximately with the molar mass of the acrylic acid monomer and could thus correspond to the molar mass for the formation of crosslinks.

5.8. Fractography

The cements made with the higher molar mass poly(acrylic acid)s and the less reactive low fluorine glasses exhibited rib markings on the fracture surfaces of their DT specimens characteristic of thermoplastics polymers, such as poly(methylmethacrylate) and rubber toughened poly(methylmethacrylate)s [48]. This provides further support for fracture taking place through a well defined plastic zone at the crack tip and supports the calculated plastic zone size data.

6. Conclusions

Despite the fact that the reptation-chain pull-out model does not fit the observed data, the results demonstrate the dominant influence of poly(acrylic acid) molar mass on cement properties. The polymer molar mass is the dominant factor at all three time intervals. It has been suggested that the formation of a silicate phase accounts for the long term changes in the mechanical properties of glass polyalkenoate cements and that the role of the poly(acrylic acid) is to confer strength and toughness only during the early stages of the setting reaction [23]. The results indicate a dominant influence of the poly(acrylic acid) molar mass even at 28 days. The application of the reptation chain pull-out model to glass polyalkenoate cements has been criticised [50, 51], but is currently the only available model for analysing the fracture behaviour that is capable of making quantitative predictions [52]. The dependance of toughness on molar mass decreases markedly with time and with glass reactivity. At short times after setting and with less reactive glasses, the slope is close to one. However, at longer times after setting, the more reactive glasses give slopes below 0.5 and below that found for the previous commercial glass at one day. The dominant role poly(acrylic acid) exerts on fracture toughness, un-notched fracture strength and compressive strength, even at cement ageing times of 28 days points to the silicate phase having a minor contribution. The increases in Young's modulus, as well as reductions in toughness and plasticity at the crack tip with time are more consistent with increased crosslinking of the polyacrylate chains by metal cations.

One of the major advantages of glass polyalkenoate cements is their ability to release fluoride ions. Their major deficiency is their poor fracture toughness. Whilst the fracture toughness has been increased dramatically, this is at the expense of using low or fluorine free glasses. Previous studies have demonstrated a strong correlation of the fluorine content of the glass with the amount of fluoride released from the set cement [53]. Thus the cements with the high fracture toughness values will not release fluoride ions in large amounts. Despite this drawback, it is thought that significant improvements in fracture toughness and toughness can be obtained by moving to a poly(acrylic acid) with a molar mass above that of E9, but below that of E11 and increasing the polyacid concentration. Recent studies [54] have demonstrated that cement properties improve dramatically with poly(acrylic acid) concentration. The E11 material has a molar mass distribution in which some of the chains are so long that they are probably above M_c and in the plateau region (Fig. 5), where toughness is independent of molar mass. These chains will not contribute any additional toughness, but will contribute to an even higher viscosity. Since the viscosity would be expected to scale as the molar mass raised to the power 3.0 [9] excessively long chains are to be avoided. Long chains will contribute disproportionately to the viscosity and not so dramatically to the toughness. Optimisation of the molar mass distribution should enable the poly(acrylic acid) concentration to be increased and further increases in the fracture toughness to be obtained. Whilst the fracture toughness has been increased significantly compared to existing commercial materials, the fracture toughness is still significantly below that of the structural component of tooth, dentine at 2.4 MPa $m^{1/2}$.

Frequently the compressive strength of glass polyalkenoate cements is the only mechanical property to be evaluated and this parameter is usually only measured at one day. It can be seen that the linear elastic fracture mechanics approach gives a much greater insight into failure in these materials. Furthermore, compressive strength as a parameter is relatively insensitive to the changes that occur with time in these dynamic materials. For example, whilst the Young's modulus changes markedly with time, compressive strength often remains approximately constant. Further long term studies are required with these cements in order to optimise their properties and performance.

Acknowledgements

The authors would like to thank Allied Colloids Bradford (UK) for supply of the poly(acrylic acid)s and Dr Malcom Hawe for the gel permeation chromatography data. Richard Billington AHC/Shofu for supply of the medical grade poly(acrylic acid) "E9" the European Commission for funding under the Brite EuRam Scheme Project No BE6062 Contract No BRE2.CT92.0349. Finally the authors would like to acknowledge research staff from ESPE (Germany) Dentsply (Germany) and PSP Dental (UK) for their comments and help during the course of this study.

References

1. R. G. HILL and A. D. WILSON, *Glass Technol.* **29** (1988) 150.
2. S. GRIFFIN and R. HILL, *J. Non-Cryst. Solids* **196** (1996) 255.
3. R. G. HILL, *J. Mater. Sci. Letts.* **8** (1989) 1043.
4. R. G. HILL, C. P. WARRENS and A. D. WILSON, *J. Mater. Sci.* **24** (1989) 363.
5. A. D. WILSON, R. G. HILL, C. P. WARRENS and B.G. LEWIS, *J. Dent. Res.* **68** (1989) 89.
6. R. G. HILL, *J. Mater. Sci.* **28** (1993) 3851.
7. J. P. BERRY, *J. Polym. Sci.* **50** (1961) 313.
8. J. P. BERRY, *SPE. Trans* **1** (1961) 1.
9. P. G. DE GENNES (Cornell University Press, New York, 1979).
10. P. G. DE GENNES, *Physics Today* June (1983) 344.
11. P. PRENTICE, *Polymer* **24** (1983) 344.
12. G. L. PITMAN and I. M. WARD, *ibid.* **20** (1979) 895.
13. K. JUD, H. H. KAUSCH and J. G. WILLIAMS, *J. Mater. Sci.* **16** (1981) 204.
14. H. H. KAUSCH and K. JUD, *Plast. Rub. Process Appl.* **2** (1982) 265.
15. P. PRENTICE, *J. Mater. Sci.* **20** (1985) 1445.
16. R. J. MARTIN, J. F. JOHNSON and A. R. COOPER, *J. Macromol. Sci Rev. Macromol. Chem.* **C8** (1972) 57.
17. J. D. FERRY (Wiley, New York, 1980).
18. S. CRISP, B. G. LEWIS and A. D. WILSON, *J. Dent.* **4** (1976) 162.
19. M. A. CATTANI-LORENTE, C. G. GODIN and J. MEYER, *Dent. Mater.* **10** (1994) 37.
20. J. A. WILLIAMS, R. W. BILLINGTON, *J. Oral Rehab.* **18** (1991) 163.
21. G. PEARSON and A. ATKINSON, *Biomaterials* **12** (1991) 169.
22. E. A. WASSON and J. W. NICHOLSON, *J. Dent. Res.* **72** (1983) 481.
23. A. D. WILSON, *J. Mater. Sci. Letts.* **15** (1996) 275.
24. K. A. MILNE, N. J. CARLOS, J. H. O'CONNELL, C. H. L. KENNARD, S. VEGA and D. MARKS, *J. Mater. Sci. Mater. Med.* **8** (1997) 349.
25. S. MATSUYA, T. MAEDA and M. OHTA, *J. Dent. Res.* **75** (1996) 1920.
26. R. HILL, Fracture studies on glass-ionomer cements, Unpublished Report No 684/B14/RGH/8/86, Laboratory of the Government Chemist, 1986.
27. P. V. HATTON and I. M. BROOK, *brit. Dent. J.* **173** (1992) 275.
28. S. MATUSUYA, Y. MATUSUYA and M. OHTA, *Amer. Assoc. Dent. Res.* (Abstract) **1442** (1998).
29. A. D. WILSON and J. W. MCLEAN (Quintessence Publishing Co., Inc. 1988) Chap. 8.
30. W. ZOLLNER and C. RUDEL, in "Glass-ionomers the Next Generation," edited by P. HUNT, International Symposia in Dentistry, Philadelphia PA 19103.
31. I. M. BROOK, G. T. CRAIG and D. J. LAMB, *Clinical Materials* **4** (1991) 295.
32. I. M. BROOK, P. V. HATTON and R. HILL, *J. Mater. Sci. Materials in Medicine* **6** (1996) 690.
33. L. M. JONCK and C. J. GROBBELAAR, *Clinical Materials* **5** (1990) 323.
34. R. T. TURNER, R. FRANCIS, D. BROWN, J. GARAND, K. S. HANNON and N.H. J. BELL, *Bone Miner. Res* **4** (1989) 477.
35. M. OKAZAKI and M. SATO, *Biomaterials* **11** (1990) 573.
36. C. H. LLOYD and L. MITCHELL, *J. Oral Rehab.* **11** (1984) 257.
37. M. GOLDMAN, *J. Biomed Mater. Res.* **19** (1985) 771.
38. G. LEWIS, *J. Mat. Edu.* **12**, 1.
39. A. O. AKINMADE and R.G. HILL, *Biomaterials* **13** (1992) 931.
40. D. WOOD and R. G. HILL, *Clinical Materials* **7** (1991) 301.
41. British Standards Institution (London), Specifications for dental glass ionomer cements, BS 6039, 1981.
42. P. S. LEEVERS and J. G. WILLIAMS, *J. Mater. Sci.* **20** (1985) 77.
43. J. A. KIES and B. J. CLARKE, "Fracture" edited by P. L. PRATT (Chapman and Hall, London, 1969) p. 483.
44. ASTMS D790-1 Standard methods of test for the flexural properties of plastics (American Society of Testing and Materials, Philadelphia, 1971).
45. S. GRIFFIN, Ph.D. thesis, University of Limerick, August, 1996.
46. M. THOMAS, University of Greenwich, Unpublished results.
47. R. G. HILL and S. LABOK, *J. Mater. Sci.* **27** (1992) 67.
48. R. HILL, *ibid.* **11** (1994) 3062.
49. J. W. NICHOLSON, *J. Mat. Sci. Mater. in Medicine* **3** (1992) 157.
50. J. W. NICHOLSON, *J. Mater. Sci. Letts.* **12** (1993) 808.
51. R. G. HILL, *ibid.* **12** (1993) 332.
52. R. G. HILL, E. DE BARRA, S. GRIFFIN, G. HENN, P. V. HATTON, A. J. DEVLIN, K. K. JOHAL and I. M. BROOK, *Key Engineering Materials* **99–100** (1995) 315.
53. E. DE BARRA, Ph.D. thesis, University of Limerick, in preparation.

Received 13 March
and accepted 21 August 1998